Morphology, Thermal and Mechanical Properties of the Polyhedral Oligomeric Silsesquioxane Side-Chain Epoxy Hybrid Material

Yie-Chan Chiu,[1] I-Chen Chou,[1] Hsieh-Chih Tsai,[2] Linawati Riang,[1] Chen-Chi M. Ma[1]

[1]*Department of Chemical Engineering, National Tsing-Hua University, Hsin-Chu, Taiwan 30043, Republic of China*
[2]*Graduate Institute of Engineering, National Taiwan University of Science and Technology, Taipei 116, Taiwan, Republic of China*

Received 27 March 2009; accepted 3 May 2010
DOI 10.1002/app.32752
Published online 15 July 2010 in Wiley InterScience (www.interscience.wiley.com).

ABSTRACT: The side-chain polyhedral oligomeric silsesquioxane (POSS)-type epoxy (IPEP) hybrid material was synthesized, and the particle sizes of the POSS segment were less than 5 nm and which particles dispersed uniformly. The 3D AFM microphotograph of the IPEP/DGEBA (diglycidyl ether of bisphenol A) hybrid material exhibited the unique "island" shape, and their XRD pattern displayed amorphous halo structure. The POSS segments of the IPEP could improve the thermal degradation activation energies. Additionally, introduction of the IPEP into the DGEBA could improve the char yield and provide the antioxidation property in the air atmosphere. The char yields of the IPEP/DGEBA hybrid materials could improve from 14.48 to 19.21% and from 0.18 to 1.17% in the nitrogen and air atmospheres, respectively. The IPEP segments could also improve the hardness when the IPEP contents of the IPEP/DGEBA hybrid materials were less than 50 wt %. © 2010 Wiley Periodicals, Inc. J Appl Polym Sci 118: 3723–3732, 2010

Key words: epoxy; POSS; nanocomposite; thermal properties

INTRODUCTION

Epoxy resin is the most important thermosetting material; it has been widely used as the adhesives, electronic encapsulating compounds, coatings, etc. The epoxy resins could also serve as the matrix for various nanocomposites and be used for the structural materials. Because of the cured epoxy materials possess high modulus and strength, excellent chemical resistance.[1] Recently, many researches focused on the improvement of the thermal properties and flame retardancy of the epoxy materials.[2–5] Introduction of various halogen atoms into the epoxy resins was the conventional method to improve the thermal stabilities. However, for the environmental and health considerations, the halogenated components were restricted. Consequently, some alternatives containing phosphorus, silicon, and nitrogen moieties were used.[2–5]

Introduction of various inorganic materials into the polymer has been studied, which associated with incorporating the inorganic building blocks on nanoscale and preparing various polymer-based materials. The polymer/inorganic nanocomposites possess various characteristic properties; these properties can continue to be a driving force for the new materials development.[6–8] The novel chemical material for the nanoreinforced and new organic/inorganic hybrids materials could be prepared by the polyhedral oligomeric silsesquioxanes (POSSs). The POSS exhibited the nanosized cage architecture and which structure possessed Si—O—Si framework. Its empirical formula is $(RSiO_{1.5})_n$, where n is an even number (6,8,10,. . .) and R is an organic substituent (typically methyl, halogen, vinyl, or phenyl). However, unlike silica, silicones, and other fillers, the POSS molecule contains either nonreactive or reactive organic substituent at the corner of the POSS cage architectures. The POSS features the unique and large molecules. The POSS particle is $\sim$ 1–3 nm in size compared with the polymer segments.[9–14]

The incorporation of the POSS into polymeric materials could result in the polymer properties improvement. The enhanced properties include good mechanical properties, excellent thermal stability, lower oxygen permeability, lower thermal conductivity, lower thermal expansion, lower dielectric permittivity, and lower surface energy. Recently, there were several investigations for the organic–inorganic epoxy/POSS nanocomposites.[15–21] Lee and Lichtenhan[15] investigated the thermal and viscoelastic properties of the epoxy/POSS nanocomposite and found that the POSS could retard the physical aging process in the glassy state. Liu et al.[16,17] used the small-molecule curing agents to prepare the epoxy/POSS hybrid materials, and the macrophase

Correspondence to: C.-C. M. Ma (ccma@che.nthu.edu.tw).

separation was not observed in the investigation. Zheng and coworkers[18–21] investigated the morphology, thermomechanical and thermal properties of the series of the epoxy/POSS nanocomposites, and the POSS of the epoxy/POSS nanocomposites possessed various organic R groups.

In this work, the isocyanatopropyldimethylsilyl-isobutyl-POSSs-type epoxy (IPEP) was synthesized from the isocyanatopropyldimethylsilyl-isobutyl-POSS (IPI-POSS) and the DGEBA (diglycidyl ether of bisphenol A) epoxy. And, the various IPEP/DGEBA hybrid materials were prepared. The POSS-dispersed morphology was investigated by the SEM, EDX, TEM, and XRD. The thermal degradation properties of the IPEP/DGEBA hybrid materials were investigated by the TGA. The thermal degradation activation energies of the IPEP/DGEBA hybrid materials were determined by the Ozawa's and Kissinger's methods. The hardness of the IPEP/DGEBA hybrid materials was studied by the Shore D.

EXPERIMENTAL

Materials

The diglycidyl ether of bisphenol A epoxy resin, with an epoxy equivalent weight (EEW) of 180 g/equiv, was obtained from the Nanya Plastics, Taiwan. The isocyanatopropyldimethylsilyl-isobutyl-POSS (IPI-POSS, ICO655) possessed seven isobutyl groups and one isocyanates group and obtained from the Hybrid Plastics, MS, USA. The 4,4′-methylenedianiline (DDM) was used as the curing agent and obtained from the Acros Organic, Geel, Belgium. The tetrahydrofuran (THF) was obtained from the Tedia, Fairfield, OH. The tin chloride dehydrate ($SnCl_2$) used as the catalyst and obtained from the Showa Chemical, Tokyo, Japan.

Instrumental methods

The FTIR analysis of the cured hybrid materials was measured with the Perkin–Elmer Spectrum One FTIR (MA, USA), which equipped with an attenuated total reflectance (ATR) accessory. Thermogravimetric analysis (TGA) was conducted with a Thermal Analyzer TGA-951 at different heating rates under the nitrogen and air atmospheres. The gas flow rate was 100 ml/min. Differential scanning calorimetric (DSC) thermograms were recorded with a Thermal Analyzer DSC-Q10 at an optimum heating rate of 10°C/min under nitrogen atmosphere. The nitrogen gas flow rate was 50 mL/min. The DSC and TGA were provided from Waters (MA, USA). The characterization of the IPEP/DGEBA hybrid materials structures were investigated by the D/max 2400 X-ray diffractometer (Cu kα radiation). The X-ray generator settings were 40 kV and 35 mA, and the scanning range was acquired from 5° to 40°. The LOI instrument determined the flame retardant property, which with an Atlas limiting oxygen index (LOI, ATLAS Fire Science Products, NY, USA). Chamber accorded to the standard procedure (ASTM D 2836) with test specimen bar. The LOI represented the lowest oxygen content for sustaining the flame. The oxygen content required at ambient atmosphere is about 21%. Generally, the composites LOI values higher than 26 could show self-extinguishing behavior and consider as high flame retardance. Atomic force microscopy (AFM) measurements were carried out with the AFM Seiko SPI3800N, series SPA-400 (Tokyo, Japan).

The morphology of the fracture surface of the hybrid material was examined by a scanning electron microscope (SEM) of JEOL JSM-5300 (Tokyo, Japan). The fracture surfaces of the IPEP/DGEBA hybrid materials were plated with gold. Transmission electron microscope (TEM) JEOL JEM-1230 (Tokyo, Japan) was performed with an accelerating voltage of 100 kV. The IPEP/DGEBA hybrid materials were trimmed into 100-nm-thick slices in the direction parallel to the plane of the films. Shore D was used to measure the hardness of the IPEP/DGEBA hybrid materials. The PTC Instrument Type D Durometer, Model 307L (Los Angeles, USA) was used for hardness testing. The Shore D hardness test was carried out according to ASTM D 2240. The degree of angle of hardness testing is 90°.

Preparation of the POSS side-chain–type epoxy resin (IPEP)

The DGEBA epoxy resin (10 g) and the isocyanatopropyldimethylsilyl-isobutyl-POSS (2 g, IPI-POSS) were dissolved into the tetrahydrofuran (15 g, THF) to form a homogeneous solution. All of the reactants were in the 50-mL glass reactor equipped, and the reaction system possessed a thermometer, reflux condenser, and stirrer. Tin chloride dehydrate ($SnCl_2$) was used as catalyst and added into this reaction system. The homogeneous solution was stirred at 60–70°C for 8–10 h. Then, the homogeneous solution was concentrated with the rotary evaporator, and the light white viscous product was obtained with 100% yield. The preparation of the IPEP is described in Scheme 1. The $HClO_4$/potentiometric titration method was used to determine the equivalent weight (EEW) of the IPEP. The EEW of the IPEP was about 1063 g/equiv.

Preparation of the IPEP/DGEBA hybrid materials

The IPEP/DGEBA hybrid materials were prepared from various weight ratios of the IPEP and DGEBA.

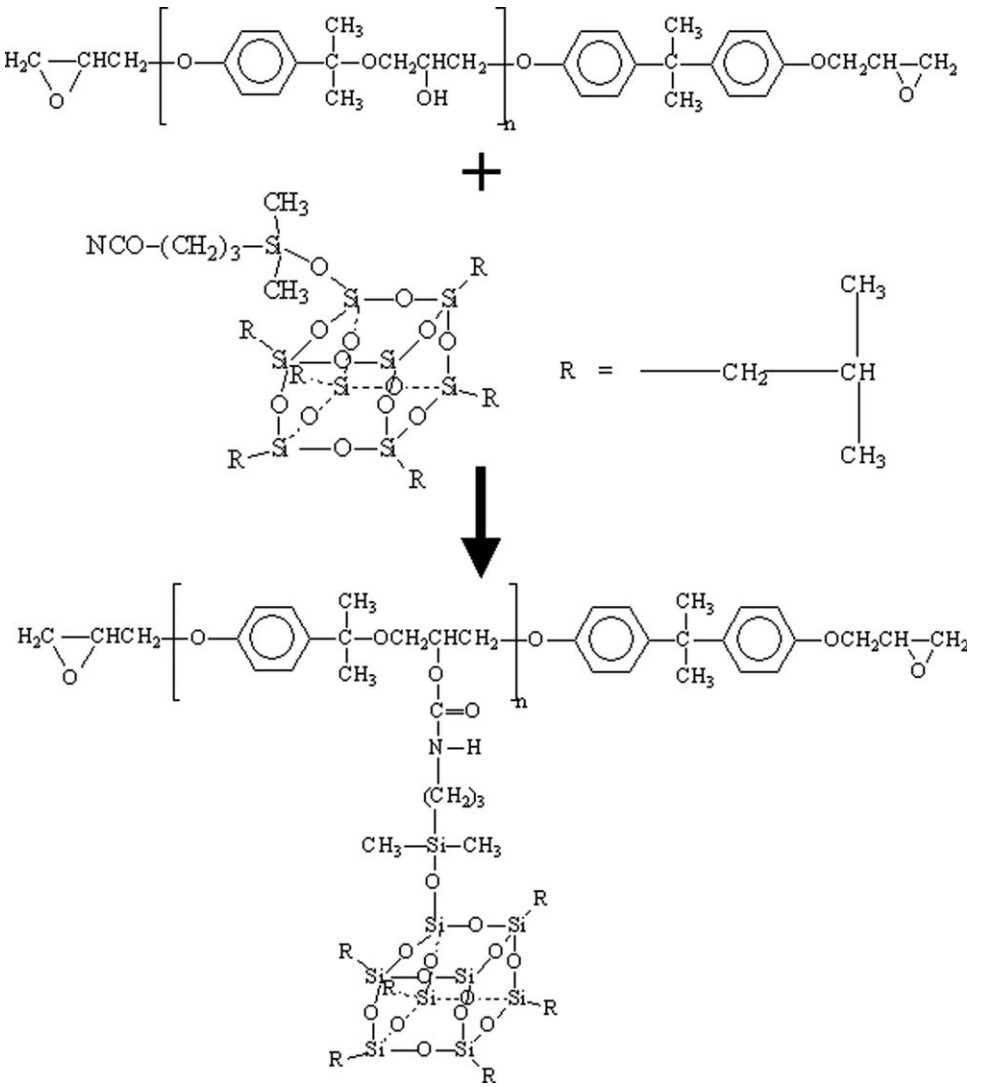

Scheme 1 Synthesis of the IPI-POSS-modified epoxy (IPEP).

For the IPEP5 hybrid material, the reaction system possessed the DGEBA epoxy (9.5 g) and the IPEP reactant (0.5 g). This IPEP/DGEBA hybrid material possessed 5 wt % of the IPEP. All of the IPEP/DGEBA hybrid materials were prepared from DGEBA, IPEP, and DDM. For the IPEP50, the reactant molar ratios of the DGEBA, IPEP, and DDM were 1.05 : 1.05 : 1, respectively. The IPEP0 was the pristine-cured DGEBA/DDM materials, without any IPEP (POSS) contents. All of the reactants were solved into the THF. The solvent was removed under vacuum at room temperature for 24 h, and the residual was heated continuously at 80°C (2 h), 120°C (2 h), 160°C (4 h), and 180°C (6 h). Table I presents the IPEP (POSS) weight ratios of various IPEP/DGEBA hybrid materials.

Figure 1 presents the ATR spectra of the IPEP/DGEBA hybrid material. The characteristic bands at 3291 and 1625 cm^{-1} were associated with the N—H bonding of the amine curing agent and urethane-like group. The characteristic bands of the carbonyl (C=O) and the N—C bonding were appeared at 1726 and 1196 cm^{-1}, respectively. The Si—O—Si bonding of the POSS exhibited two characteristic peaks, which associated with 1051 and 1031 cm^{-1}, respectively. The characteristic peaks of the aromatic ring were showed at 1608, 1481, and 1461 cm^{-1}, respectively.

Kinetic studies of the thermal degradation process

Ozawa's method[22]

The degree of thermal degradation, α, is defined in eq. (1)

$$\alpha = \frac{m_0 - m}{m_0 - m_\infty}, \quad (1)$$

where m_0 is the initial weight, m is the weight at temperature T, and m_∞ is the weight at the end of experiment. The Ozawa's equation is defined as:

TABLE I
The IPEP (POSS) Weight Ratios of Various IPEP/DGEBA Hybrid Materials

Code	IPEP contents (wt %)	DGEBA contents (wt %)	POSS contents (wt %)
IPEP0	0	100	0.00
IPEP5	5	95	0.83
IPEP10	10	90	1.67
IPEP30	30	70	5.00
IPEP50	50	50	8.34
IPEP70	70	30	11.67
IPEP90	90	10	15.00

$$\log \beta = -0.4567\left(\frac{E_a}{RT}\right) + \left[\log\frac{AE_a}{R} - 2.315 - \log F(\alpha)\right], \quad (2)$$

where E_a is the thermal degradation activation energy, R is the ideal gas constant, T is the absolute temperature of various conversion degrees of thermal degradation, and β is the heating rate. The thermal degradation activation energy was obtained from the plot of lnβ vs. $1/T$ for each value of α.

Kissinger's method[23]

The Kissinger's method is shown in eq. (3)

$$\frac{d\left[\ln\left(\beta/T_m^2\right)\right]}{d(1/T_m)} = -\frac{Ea}{R} \quad (3)$$

where T_m is the maximum temperature of the first derivative weight loss curves. The β is the heating rate and R is the ideal gas constant. The thermal degradation activation energy can be determined from the plot of $\ln(\beta/T_m^2)$ vs. $1/T_m$.

RESULTS AND DISCUSSION

The morphology of the IPEP/DGEBA hybrid materials

The morphology of the fracture surface of the IPEP70 hybrid material was investigated by the SEM, and Figure 2 presents the SEM microphotograph of the IPEP70 hybrid material. The fracture surface was smooth and without any microphase separation. Additionally, the inorganic segments (POSS) were dispersed homogeneously throughout the epoxy matrix. All of the reactants (DGEBA, DDM, and IPI-POSS) were well mixed on the nanometer scale,[24,25] and which smooth surface was uniform. Hsiue et al.[26] indicated that the uniform smooth surface associated with the long methylene chain and network chain could move easily. The side chains of the IPEP/DGEBA hybrid materials were the IPI-POSS bulky segments, and these bulky side groups may increase free volume. The chain movement of the network occurred easily and to take place in the homogeneous-cured hybrid materials. The distributions of the POSS segments in the epoxy matrix were studied by the SEM-EDX Si-mapping analysis. Figure 3 is the Si-mapping microphotograph of the IPEP/DGEBA hybrid material. The white dots represent each silicon atoms. The POSS segments dispersed uniformly throughout the epoxy matrix.[27] The inorganic segments (POSS domain) without any aggregated therein.

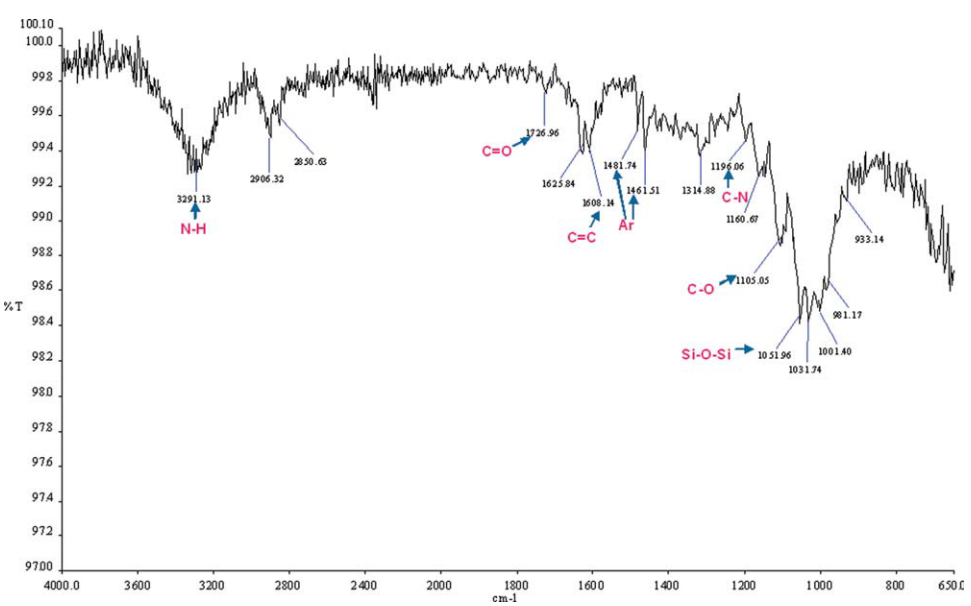

Figure 1 The ATR spectra of 70 wt % IPEP hybrid material (IPEP70). [Color figure can be viewed in the online issue, which is available at www.interscience.wiley.com.]

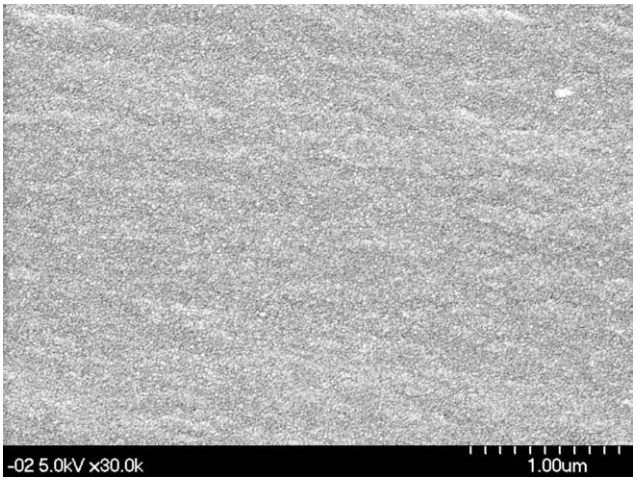

Figure 2 The SEM microphotograph of 70 wt % IPEP/DGEBA hybrid material (IPEP70).

Figure 4 presents the TEM microphotograph of the IPEP70 hybrid material. Laine and coworkers found that the electron density and electron beam damage differed between the organic and inorganic segments.[11] Therefore, the sample did not have to be stained. The POSS segments cluster can be observed directly in the TEM microphotograph.[11] The black dots in Figure 4 represent the POSS particles (inorganic segments), and these particles sizes are smaller than 5 nm (the scale bar represents 20 nm). The organic and inorganic segments of the IPEP/DGEBA hybrid materials are distributed uniformly on the nanoscale. Consequently, the TEM microphotographs revealed without any phase separation.[28–30]

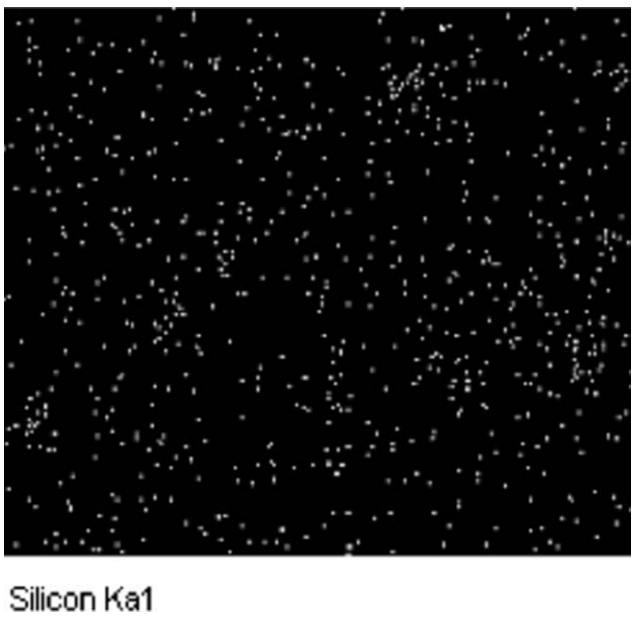

Figure 3 The Si-mapping microphotograph of 70 wt % IPEP/DGEBA hybrid material (IPEP70).

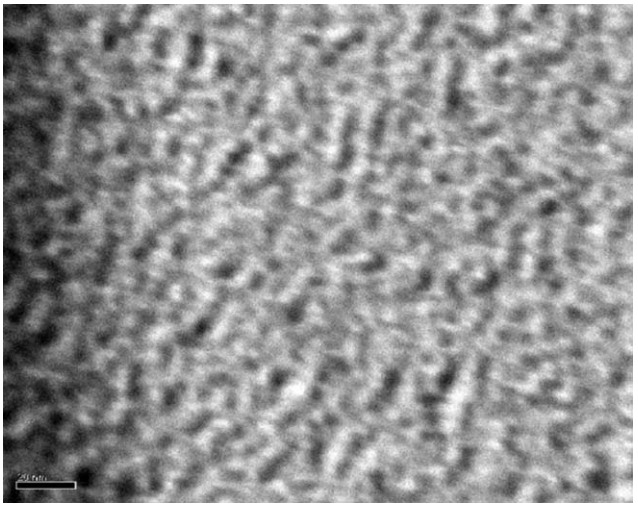

Figure 4 The TEM microphotograph of 70 wt % IPEP/DGEBA hybrid material (IPEP70, scale bar: 20 nm, 300 k).

The XRD was adopted to characterize the structure of various IPEP/DGEBA hybrid materials. Figure 5 presents the XRD patterns of various IPEP/DGEBA hybrid materials. The pristine IPI-POSS exhibits two characteristic peaks at $2\Theta = 8°–9°$ and $2\Theta = 19°$, respectively, and this phenomenon suggested the rhombic chemical structure of the IPI-POSS. However, the remaining IPEP/DGEBA hybrid materials were amorphous and yielded a broad peak at $2\Theta = 14°–15°$. As the chain entanglement and random crosslinking network structures were formed in the epoxy/amine curing reaction. Mather and coworkers found that copolymerization may retard the crystallization of the POSS segments.[31] Therefore, all of the IPEP/DGEBA hybrid materials exhibited the amorphous halo structure, and the characteristic peaks of the IPI-POSS disappeared.

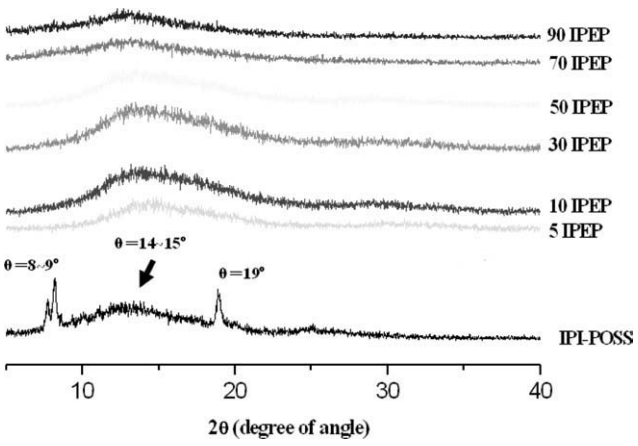

Figure 5 The XRD patterns of various IPEP/DGEBA hybrid materials.

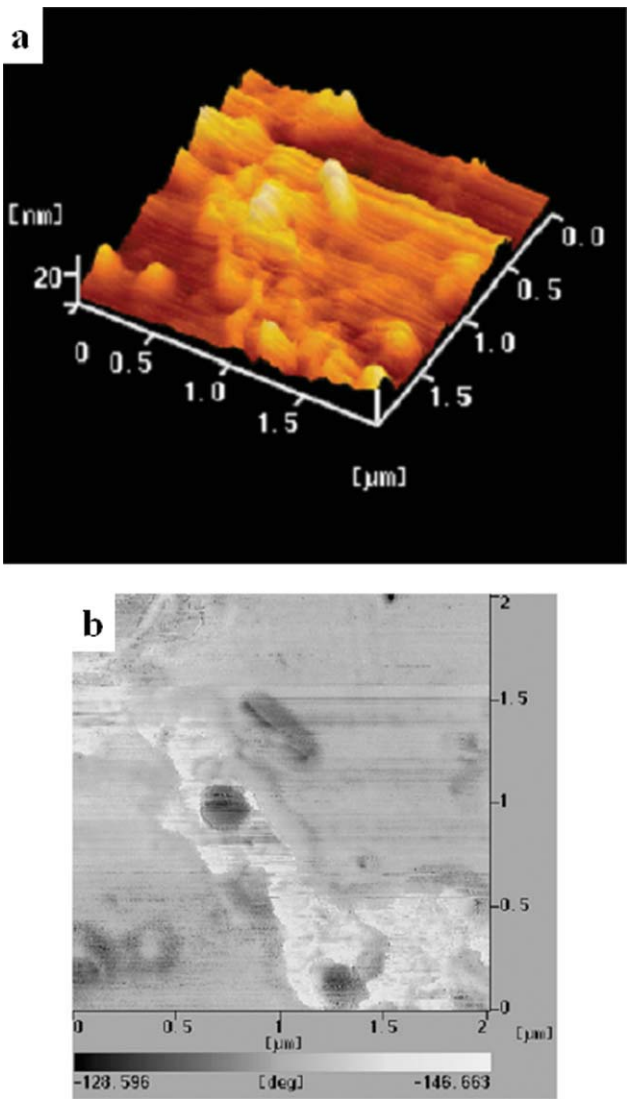

Figure 6 The AFM microphotographs of 70 wt % IPEP/DGEBA hybrid material (IPEP70): (a) the topography 3D image and (b) the phase image. [Color figure can be viewed in the online issue, which is available at www.interscience.wiley.com.]

The surface morphology of the IPEP70 hybrid material was studied by the AFM. Figure 6(a,b) presents the topographic 3D image and phase image of the IPEP70 hybrid material, respectively. The topography 3D image illustrates that the surface protrusions were responsible for surface roughness, which associated with the inorganic POSS segments. The POSS side chain could integrate to form the "island" shape and also increase the roughness of the material surface.[32–34] Furukawaet al. found that the "island" or "sea island" structure may explain by the higher cohesive energy of the polysiloxane segments.[33] Therefore, the degree of roughness of the IPEP/DGEBA hybrid materials surface may increase with the POSS contents. The phase images indicate that the POSS segments are homogeneous, and the inorganic segments were shorter than 100 nm.[35–36]

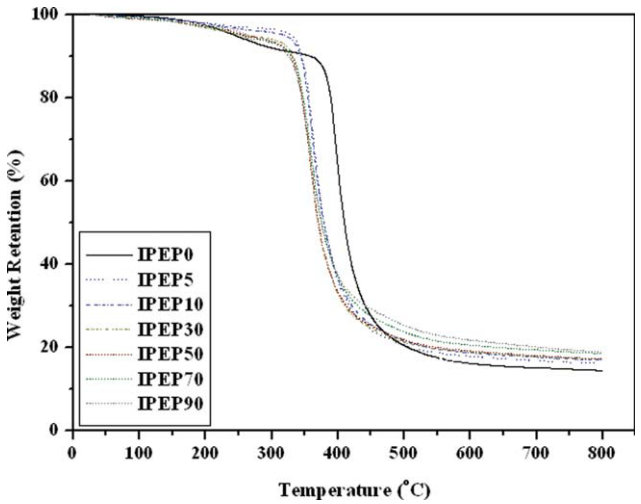

Figure 7 The TGA traces of various IPEP/DGEBA hybrid materials in nitrogen atmosphere. [Color figure can be viewed in the online issue, which is available at www.interscience.wiley.com.]

Thermal decomposition properties of the IPEP/DGEBA hybrid materials

The thermal decomposition properties of the IPEP/DGEBA hybrid materials were studied by the TGA in the nitrogen and air atmospheres. These data are presented in Figures 7 and 8; meanwhile, the T_{d5} values and char yields are summarized in Table II. In the nitrogen atmosphere, the IPEP/DGEBA hybrid materials exhibited single-step thermal degradation stage, and the T_{d5} values of the IPEP/DGEBA hybrid materials were exceeded that of the pristine-cured DGEBA/DDM material (IPEP0). Lower than 200°C, all of the IPEP/DGEBA hybrid materials

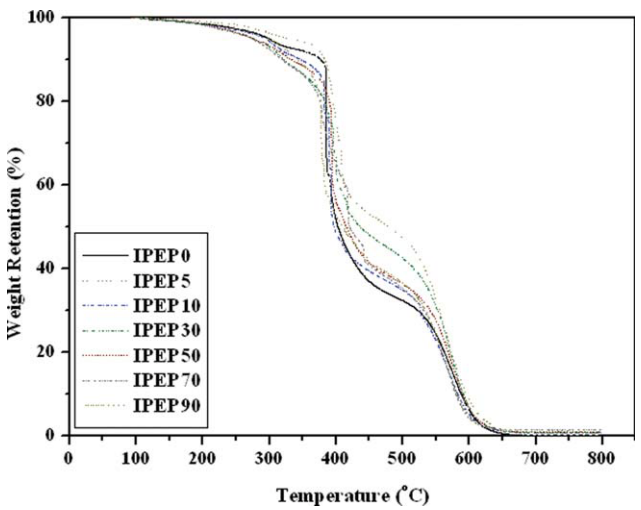

Figure 8 The TGA traces of various IPEP/DGEBA hybrid materials in air atmosphere. [Color figure can be viewed in the online issue, which is available at www.interscience.wiley.com.]

TABLE II
The Thermal Degradation Properties of Various IPEP/DGEBA Hybrid Materials

	Nitrogen atmosphere		Air atmosphere	
IPEP (wt %)	T_{d5}	Char yield (800°C)	T_{d5}	Char yield (800°C)
0	246.42	14.48	299.47	0.18
5	329.98	16.20	334.24	0.70
10	320.97	17.02	294.61	0.81
30	262.29	17.28	277.46	0.89
50	255.55	17.29	277.40	0.91
70	254.86	18.61	268.43	1.14
90	268.14	19.21	298.52	1.17

exhibited a stage of thermal degradation (a little weight loss) in the nitrogen atmosphere, which resulted from the cured materials possessed a little water. Notably, T_{d5} decreased with the IPEP contents between 30 and 90 wt %. As the IPEP side chain possessed the urethane-like side-chain linkages, which exhibited lower thermal stability than the DGEBA chemical structure. Therefore, the nanoreinforcement effect of the POSS was not sufficiently strong to inhibit the thermal decomposition of the urethane-like side-chain linkages when high IPEP contents were introduced. Additionally, the bulky POSS side chains of the IPEP could interfere with the epoxy/amine curing reaction; this phenomenon could improve the unreacted epoxy or amine reactants contents and generate the oligomers. Strachota et al.[37] indicated that the POSS could induce the steric effect in the epoxy/amine curing reaction, and the low mobility of the POSS-bound epoxide units might reduce efficiency of the reactive approach, and these could disturb the epoxy/amine curing reaction. Chen et al.[10] found that the unreacted epoxy or amino groups might decrease the initial thermal degradation temperature. Xiao et al.[38] indicated that the low thermal decomposition temperature might result from the unreacted curing agent groups; these curing agent groups could evaporate at lower temperature than the cured epoxy materials. Consequently, the T_{d5} values of the IPEP/DGEBA hybrid materials decreased with the IPEP contents increased. However, the char yields at 800°C increased with the IPEP content, and the char yields could improve from 14.48 to 19.21% and from 0.18 to 1.17% in the nitrogen and air atmospheres, respectively, which suggested that the silicon contents (POSS) increased and decreased the volatile fraction of the IPEP/DGEBA hybrid material. Additionally, the silicon migrated to the surface of the IPEP/DGEBA hybrid materials and acted as a barrier to protect the polymer from dramatic thermal degradation.[3,39] Liu and coworkers found that the silicon is a char protector, rather than a promoter of the char formation.[3] All of the IPEP/DGEBA hybrid materials exhibit two stages of the thermal degradation in the air atmosphere, and the second stage is the thermal oxidation stage. Figure 9 indicates that incorporation of the IPEP segments could slow down the thermal oxidation between 400 and 600°C, as the silica char could form the thermal insulation and provide an antioxidant effect at high temperature range.[40–41] Zhang et al.[42] found that the POSS architectures are thermally resistant; however, the steric hindrance of the POSS segments impedes the molecular chain movement and destroys the crosslinking degree of the epoxy/amine curing reaction.

From Figure 9, when the IPEP contents are lower than 50 wt %, the LOI values of the IPEP/DGEBA hybrid materials are increased with the IPEP contents. The inorganic nanosilica segments could improve the thermal stability. These inorganic silica char formations could improve the flame retardant properties. However, the LOI values of the IPEP/DGEBA hybrid materials are decreased with the IPEP contents when the IPEP contents are higher than 50 wt %. As the high IPEP contents could inhibit the epoxy/amine curing reaction. The bulky POSS side-chain segments of the IPEP could interfere with the curing reaction and cause the improvement of the oligomers. Additionally, the IPEP

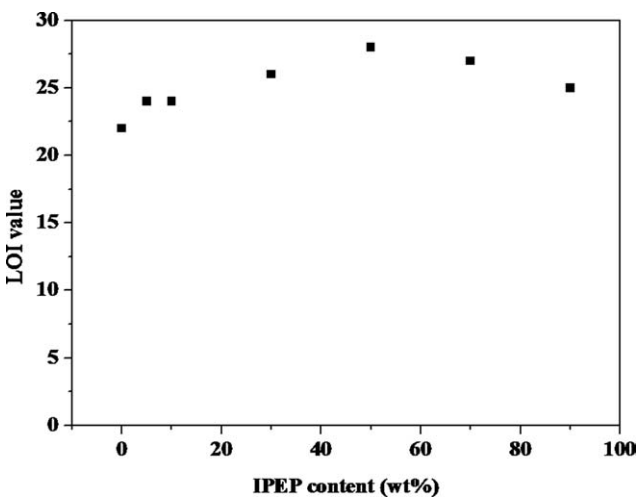

Figure 9 The LOI values of various IPEP/DGEBA hybrid materials.

segments possessed *i*-butyl organic groups of the POSS and the urethane-like side-chain linkages. The high oligomers, *i*-butyl organic groups, and the urethane-like side-chain linkages contents could improve the flammability. Consequently, the LOI values are decreased with the IPEP contents when the IPEP contents are higher than 50 wt %.

The thermal degradation activation energies of the IPEP/DGEBA hybrid materials

The thermal degradation activation energies (E_as) were calculated by the Ozawa's method.[22] Figures 10 and 11 illustrate the E_as extent of thermal degradation under the nitrogen and air atmospheres, respectively. When the IPEP/DGEBA hybrid materials were heated, the thermal stable silica could migrate to the surface of the IPEP/DGEBA hybrid materials. Zhang et al.[43] found that the POSS thermal decomposition could form the thickness of inert layers, and these layers increased with the POSS contents. Meanwhile, the increase of the POSS contents could enhance the thermooxidation degradation resistance of the POSS/epoxy hybrid materials. In the air atmosphere, Liu and Chou[44] also found that the POSS decomposed and generated the silica-like layer; this phenomenon could prevent the epoxy materials from thermal degradation dramatically. Notably, the thermal degradation activation energies did not vary greatly with some thermal decomposition conversion, as the complex thermal degradation mechanisms of the POSS/epoxy were described by a single empirical kinetic model.[45–2] From the TGA pattern (Fig. 8, in the air atmosphere), the second-stage thermal degradation is the stage of thermal oxidation, this stage about the degree of pyrolysis

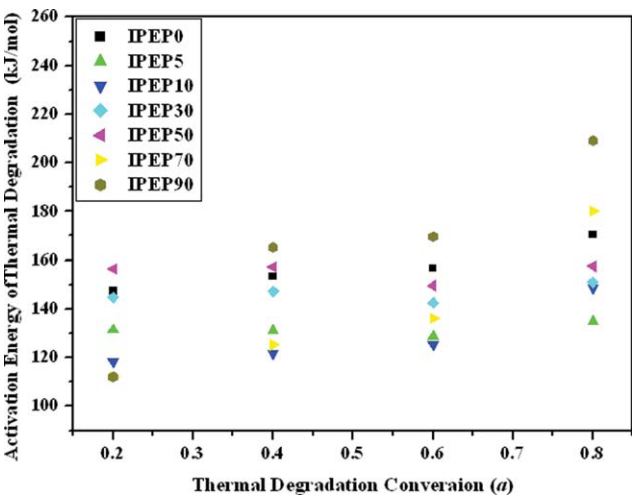

Figure 10 The activation energies of various thermal degradation conversions in nitrogen atmosphere (by Ozawa's method). [Color figure can be viewed in the online issue, which is available at www.interscience.wiley.com.]

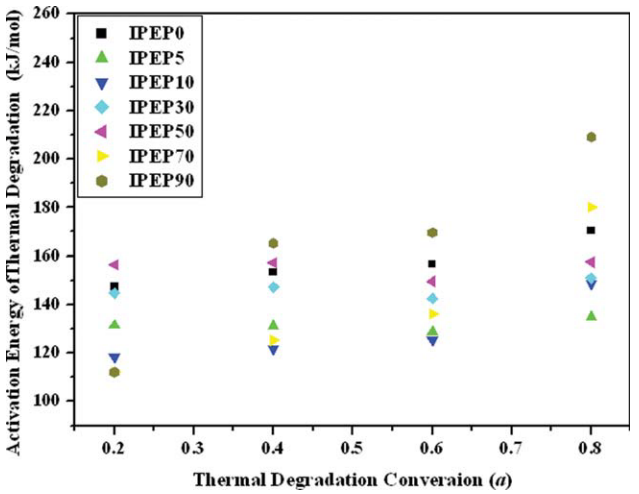

Figure 11 The activation energies of various thermal degradation conversions in air atmosphere (by Ozawa's method). [Color figure can be viewed in the online issue, which is available at www.interscience.wiley.com.]

(α) 0.35–0.73. The oxygen acted as a catalyst in the thermal oxidation stage.[46] This oxygen catalyst reduced the activation energies of thermal oxidation. At high thermal degradation conversion range, the thermal stable silica char segments more effectively inhibited the thermal degradation and increased the thermal degradation activation energy of this process.

Table III presents the activation energies of the maximum thermal degradation rate stage (the maximum thermal degradation rate stage determined by the differential thermal decomposition weight loss of the TGA analysis data); these activation energies were calculated by the Ozawa's and Kissinger's methods.[22,23] Notably, the thermal degradation activation energies are increased with the IPEP contents, because of the formation of the thermally stable silica

TABLE III
The Activation Energy of Maximum Thermal Degradation Rate Stage[a]

	Nitrogen atmosphere		Air atmosphere	
IPEP (wt %)	Ozawa[b]	Kissinger[b]	Ozawa[b]	Kissinger[b]
0	159.70	165.50	98.67	138.49
5	129.25	145.86	102.76	157.11
10	130.66	151.61	106.77	160.75
30	141.80	173.89	115.29	181.05
50	148.39	178.37	127.31	193.65
70	155.25	183.23	128.63	201.71
90	193.81	200.69	134.08	281.55

[a] The maximum thermal degradation rate stage determined by the differential thermal decomposition weight loss from the TGA analysis.
[b] The unit of thermal degradation activation energy is kJ/mol.

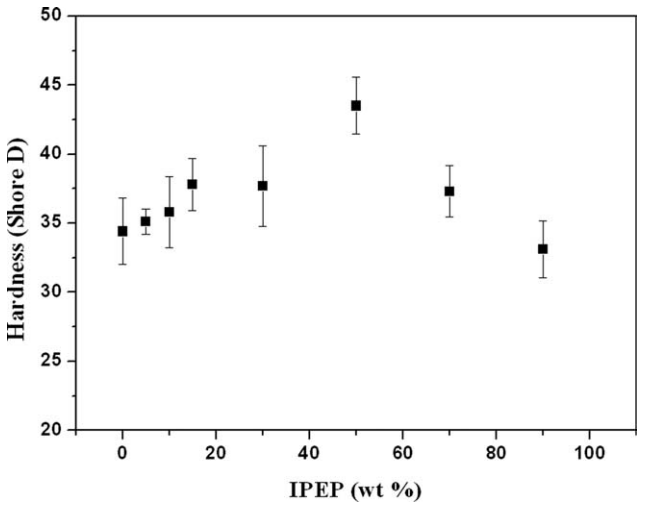

Figure 12 The hardness of various IPEP/DGEBA hybrid materials.

residue. These silica char could effectively inhibit the thermal decomposition of the IPEP/DGEBA hybrid materials both in the nitrogen and air atmospheres. However, the nanoreinforcement effect of the POSS segments might also improve the thermal degradation activation energies of the IPEP/DGEBA hybrid materials. Therefore, introduction of the IPEP components into the DGEBA epoxy could prevent the cured epoxy from thermal degradation dramatically.

Hardness property of IPEP/DGEBA hybrid materials

Figure 12 illustrates the hardness of various IPEP/DGEBA hybrid materials. When the IPEP contents were lower than 50 wt %, the hardness increased with the IPEP contents. As the inorganic silica segments (POSS) increased and covalent bonds of the inorganic POSS segments formed across the interface between the inorganic segments and organic segments.[47–48] Liu et al.[49] indicated that introduction of the inorganic segments into the polymer materials could improve the wear resistance and surface hardness of the nanocomposites. This phenomenon suggested the inseparable architecture of the nanocomposites and nanoreinforcement effect of the inorganic segments. Therefore, the IPEP segments could improve the hardness when the IPEP contents were lower than 50 wt %. However, the hardness decreased when the IPEP contents were higher than 50 wt %, because of the bulky POSS side-chain architectures and the POSS contents increased. More POSS side chains may cause the steric effect and destroy the crosslinking network structure of the curing reaction of the IPEP/DGEBA hybrid materials. This phenomenon could generate the oligomers and weaken the inseparable stiff architectures. Consequently, the hardness of the IPEP/DGEBA hybrid materials was reduced when the IPEP contents were higher than 50 wt %[49–50].

CONCLUSION

The isocyanatopropyldimethylsilyl-isobutyl-POSS-type epoxy (IPEP) was synthesized by the isocyanatopropyldimethylsilyl-isobutyl-POSS (IPI-POSS) and the DGEBA epoxy. Furthermore, the novel POSS-type side-chain hybrid materials (IPEP/DGEBA hybrid materials) were prepared by bended various weight ratios of the IPEP and DGEBA materials. The fracture surface of the IPEP/DGEBA hybrid materials was smooth and no phase separation observed. The POSS particles sizes were less than 5 nm and distributed uniformly into the IPEP/DGEBA hybrid materials. From XRD investigation, the polymer chain entanglements of the curing reaction and resulted in various IPEP/DGEBA hybrid materials architectures exhibited amorphous. The AFM microphotograph illustrated that the surface morphology of the IPEP/DGEBA hybrid materials displayed an "island" shape. Introduction of the IPEP segments into the DGEBA epoxy could improve the T_{d5} values. The char yield (800°C) of the IPEP/DGEBA hybrid materials could improve from 14.48 to 19.21% and from 0.18 to 1.17% in the nitrogen and air atmospheres, respectively. The IPEP segments improved the char yield; this improvement of the char formation could provide the thermal insulation and antioxidant stability at high degradation temperature range. Meanwhile, these thermal stable char could also inhibit the thermal degradation and improve the thermal degradation activation energies at higher thermal degradation conversion dramatically. The hardness of the IPEP/DGEBA hybrid materials could improve while the IPEP contents were lower than 50 wt % (the hardness increased from 34 to 44 by shore D test model).

References

1. Wang, H. F.; Han, W. J.; Tian, H. B.; Wang, Y. M. Mater Lett 2005, 59, 94.
2. Macan, J.; Brnardić, I.; Orlić, S.; Ivanković, H.; Ivanković, M. Polym Degrad Stab 2006, 91, 122.
3. Wu, C. S.; Liu, Y. L.; Chiu, Y. C.; Chiu, Y. S. Polym Degrad Stab 2002, 78, 41.
4. Levchik, S.; Piotrowski, A.; Weil, E.; Yao, Q. Polym Degrad Stab 2005, 88, 57.
5. Wang, X. D.; Zhang, Q. Eur Polym J 2004, 40, 385.
6. Fina, A.; Abbenhuis, H. C. L.; Tabuani, D.; Frache, A.; Camino, G. Polym Degrad Stab 2006, 91, 1064.
7. Xu, H. Y.; Kuo, S. W.; Lee, J. S.; Chang, F. C. Macromolecules 2002, 35, 8788.
8. Liu, H. Z.; Zheng, S. X. Macromol Rapid Commun 2005, 26, 196.
9. Mya, K. Y.; He, C.; Huang, J.; Xiao, Y.; Dai, J.; Siow, Y. P. J Polym Sci Part A: Polym Chem 2004, 42, 3490.

10. Chen, W. Y.; Wang, Y. Z.; Kuo, S. W.; Huang, C. F.; Tung, P. H.; Chang, F. C. Polymer 2004, 45, 6897.
11. Choi, J.; Yee, A. F.; Laine, R. M. Macromolecules 2003, 36, 5666.
12. Abad, M. J.; Barral, L.; Fasce, D. P.; Williams, R. J. J. Macromolecules 2003, 36, 3128.
13. Fu, B. X.; Namani, M.; Lee, A. Polymer 2003, 44, 7739.
14. Li, G. Z.; Wang, L.; Toghiani, H.; Daulton, T. L.; Pittman, C. U., Jr. Polymer 2002, 43, 4167.
15. Lee, A.; Lichtenhan, J. D. Macromolecules 1998, 31, 4970.
16. Liu, Y. L.; Chang, G. P.; Hsu, K. Y.; Chang, F. C. J Polym Sci Part A: Polym Chem 2006, 44, 3825.
17. Liu, Y. L.; Chang, G. P. J Polym Sci Part A: Polym Chem 2006, 44, 1869.
18. Ni, Y.; Zheng, S. X.; Nie, K. M. Polymer 2004, 45, 5557.
19. Liu, Y. H.; Zheng, S. X.; Nie, K. M. Polymer 2005, 46, 12016.
20. Ni, Y.; Zheng, S. X. Macromol Chem Phys 2005, 206, 2075.
21. Liu, H. Z.; Zheng, S. X.; Nie, K. M. Macromolecules 2005, 38, 5088.
22. Ozawa, T. Bull Chem Soc Jpn 1965, 38, 1881.
23. Kissinger, H. E. Anal Chem 1957, 29, 1072.
24. Kim, K. M.; Chujo, Y. J Polym Sci Part A: Polym Chem 2003, 41, 1306.
25. Wang, H.; Xu, P.; Meng, S.; Zhong, W.; Du, W. C.; Du, Q. G. Polym Degrad Stab 2006, 91, 1455.
26. Hsiue, G. H.; Wei, H. F.; Shiao, S. J.; Kuo, W. J.; Sha, Y. A. Polym Degrad Stab 2001, 73, 309.
27. Liu, Y. L.; Lee, H. C. J Polym Sci Part A: Polym Chem 2006, 44, 4632.
28. Liu, Y. R.; Huang, Y. D.; Liu, L. Polym Degrad Stab 2006, 91, 2731.
29. Pu, K. Y.; Zhang, B.; Ma, Z.; Wang, P.; Qi, X. Y.; Chen, R. F.; Wang, L. H.; Fan, Q. L.; Huang, W. Polymer 2006, 47, 1970.
30. Ochi, M.; Matsumura, T. J Polym Sci Part B: Polym Phys 2005, 43, 1631.
31. Wu, J.; Haddad, T. S.; Kim, G. M.; Mather, P. T. Macromolecules 2007, 40, 544.
32. Lee, R. H.; Lai, H. H. Eur Polym J 2007, 43, 715.
33. Furukawa, N.; Yamada, Y.; Furukawa, M.; Yuasa, M.; Kimura, Y. J Polym Sci Part A: Polym Chem 1997, 35, 2239.
34. Lee, Y. J.; Kuo, S. W.; Huang, W. J.; Lee, H. Y.; Chang, F. C. J Polym Sci Part B: Polym Phys 2004, 42, 1127.
35. Lin, C. H.; Feng, C. C.; He, T. Y. Eur Polym J 2007, 43, 725.
36. Liu, Y. L.; Hsu, C. Y.; Wei, W. L.; Jeng, R. J. Polymer 2003, 44, 5159.
37. Strachota, A.; Whelan, P.; Kříž, J.; Brus, J.; Urbanová, M.; Šlouf, M.; Matějka, L. Polymer 2007, 48, 3041.
38. Xiao, F.; Sun, Y.; Xiu, Y.; Wong, C. P. J Appl Polym Sci 2007, 104, 2113.
39. Hsiue, G. H.; Liu, Y. L.; Tsiao, J. J Appl Polym Sci 2000, 78, 1.
40. Liu, Y. L.; Wei, W. L.; Hsu, K. Y.; Ho, W. H. Thermochim Acta 2004, 412, 139.
41. Liu, Y. L.; Chiu, Y. C.; Chen, T. Y. Polym Int 2003, 52, 1256.
42. Zhang, Z.; Liang, G.; Ren, P.; Wang, J. Polym Compos 2007, 28, 755.
43. Zhang, Z.; Gu, A.; Liang, G.; Ren, P.; Xie, J.; Wang, X. Polym Degrad Stab 2007, 92, 1986.
44. Liu, Y. L.; Chou, C. I. Polym Degrad Stab 2005, 90, 515.
45. Montero, B.; Ramírez, C.; Rico, M.; Torres, A.; Cano, J.; López, J. Macromol Symp 2008, 267, 74.
46. Camino, G.; Lomakin, S. M.; Lazzari, M. Polymer 2001, 42, 2395.
47. Chand, N.; Jain, D. J Appl Polym Sci 2006, 100, 1269.
48. Sugimoto, H.; Daimatsu, K.; Nakanishi, E.; Ogasawara, Y.; Yasumura, T.; Inomata, K. Polymer 2006, 47, 3754.
49. Liu, S. P.; Hsu, W. L.; Chang, K. C.; Yeh, J. M. J Appl Polym Sci 2009, 113, 992.
50. Huang, J.; He, C.; Liu, X.; Xu, J.; Tay, S. S. C.; Chow, S. Y. Polymer 2005, 46, 7018.